



объединенный  
институт  
ядерных  
исследований  
Дубна

+

3473/2-80

28/7-80

E11-80-258

J.Cvach,\* V.I.Ilyushchenko, I.A.Savin,  
S.B.Vorozhtsov

**MAGNETIC FIELD CALCULATION  
OF THE NA-4 MUON SPECTROMETER**

Submitted to "Czechoslovak Journal of Physics".

---

\*On leave of absence from Institute of Physics,  
Czechosl. Acad. Sci., Prague, Czechoslovakia.

**1980**

## 1. INTRODUCTION

The NA-4 experiment is designed to extend the study of inclusive deep inelastic muon scattering to the highest energies and four momentum transfers available at the CERN SPS accelerator. It is done in collaboration of Bologna University, CERN /Geneva/, JINR /Dubna/, MPI /Münich/ and CEN /Saclay/. The experiment was proposed <sup>1/</sup> in 1974, during 1974-78 the muon spectrometer was constructed and assembled and from the end of 1978 it has been taking data.

## 2. SPECTROMETER

The NA-4 spectrometer is made from 10 identical parts - supermodules. A supermodule /see Fig.1/ consists of 32 iron discs with an outer diameter of 275 cm magnetized to saturation to provide a toroidal magnetic field. Each supermodule represents an independent detector equipped with eight planes of

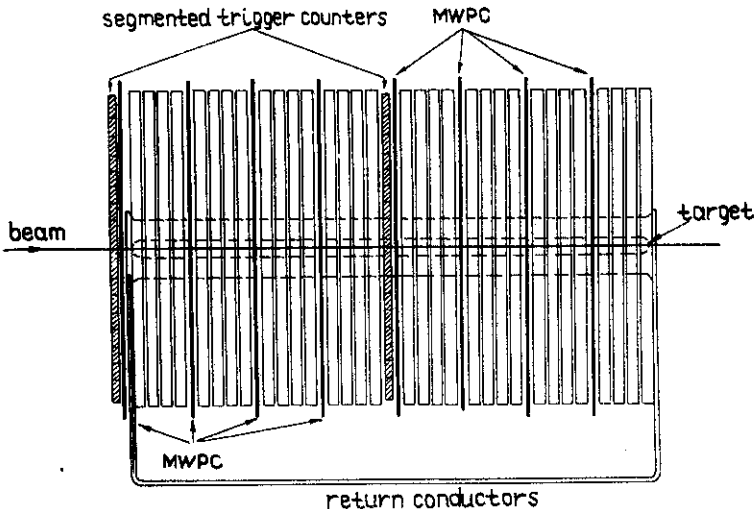


Fig.1. A schematic view of one supermodule.

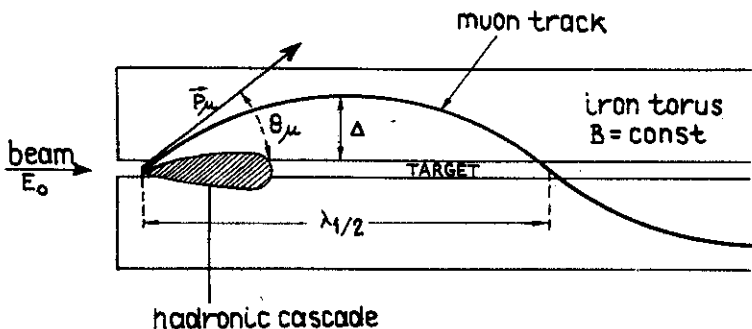


Fig.2. Muon interaction in the spectrometer.

multiwire proportional chambers with an active area of  $3 \times 3 \text{ m}^2$  and two trigger counters filled with liquid scintillator. The chambers measure alternatively  $x$  or  $y$  coordinates with a step of 4 mm. At the center of a supermodule there is a 5 m long carbon target. The scattered muon enters into the toroidal field of a supermodule and oscillates in a plane (see Fig.2) with half - wave length  $\lambda_{1/2}$  and sagitta  $\Delta$  given by

$$\lambda_{1/2} = 6.66 \frac{p_t}{B}, \quad \Delta = \frac{M_p}{0.3 B} \frac{Q^2}{Q_{\max}^2}, \quad (1)$$

(units: cm, MeV, kg), where  $p_t = p_\mu \sin \theta_\mu$ ,  $Q^2 = 2E_0 E_\mu (1 - \cos \theta_\mu)$ ,  $Q_{\max}^2 = 2E_0 M_p$ .  $E_0$  is the energy of the incident muon,  $E_\mu(p_\mu)$  the energy (momentum) of the scattered muon;  $\theta_\mu$ , the scattering angle;  $M_p$ , the proton mass;  $B$ , magnetic field induction. All other particles, except muons, are absorbed in the iron core of the magnet.

### 3. MAGNET

Each supermodule represents an independent magnetic unit with its own coil and feeder. It consists of 8 modules of 4 iron discs. An iron disc 11 cm thick has an outer radius of 137.5 cm and an inner radius of 25 cm. There is a 1.3 cm air gap between discs in a module, a 10 cm air gap between modules where a proportional chamber is inserted and a 20 cm air gap between the fourth and fifth modules where a trigger counter is placed (see Fig.1).

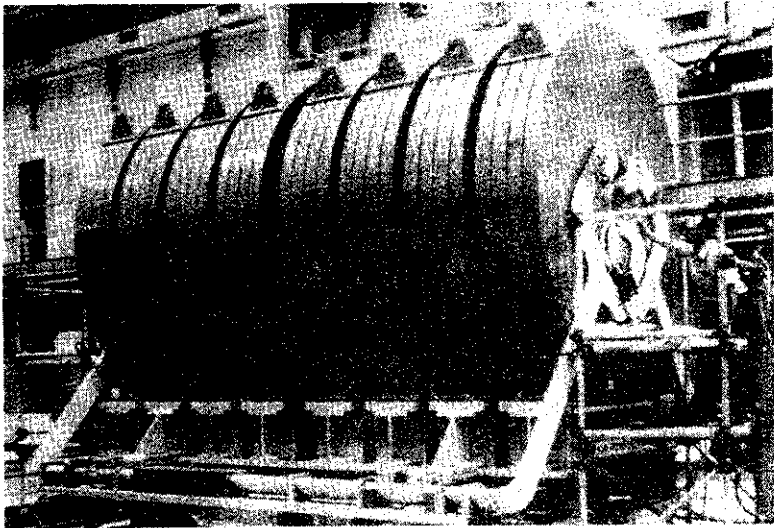


Fig.3. A view of the toroidal magnet.

The discs were manufactured of standard USSR steel of the type O8 with a low carbon content (0.06 - 0.10%). Four discs of a module are welded with the help of two stainless steel plates which are at the bottom of 45° diagonals. Two supporting legs made of standard steel are welded to the stainless steel plates. The module legs are mounted on the I profile girder (see Fig.3).

To measure the magnetic properties of iron, the discs were divided into six groups according to the carbon content. For each group a careful measurement of the magnetization curve  $B = B(H)$  was done <sup>/2/</sup> in a range of  $H = 0.5 - 330$  Oe (see Fig.4). During the assembly the discs were combined to provide the same magnetic properties of each supermodule. In calculating we used the magnetization curve for a carbon content of 0.08% which amounts to 43% of the iron discs.

The magnet coil is made from four bunches of six copper conductors placed in the hole of a supermodule on the inner surface of the iron discs at the 45° diagonals. Each wire has an oblong cross section of  $2 \times 2.5$  cm<sup>2</sup> with an inner hole for water cooling. They go parallel to the spectrometer axis, bend at the supermodule fronts and return back at a distance of 275 cm from the spectrometer axis to the feeder. Each conductor is fed by a 2500 A direct current.

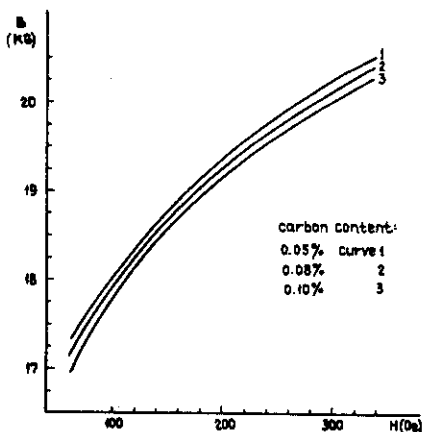


Fig.4. Magnetization curve  $B = B(H)$  for iron with a carbon content of 0.05, 0.08, 0.10%.

#### 4. METHOD OF CALCULATION

The magnetic field distribution  $B$  is given by the Maxwell equation

$$\text{rot}\left(\frac{1}{\mu}\vec{B}\right) = \frac{4\pi}{c}\vec{J}, \quad (2)$$

where  $\vec{B}$  is magnetic field induction,  $\vec{J}$  is current density and  $\mu$  is magnetic permeability. Substituting the vector potential  $\vec{A}$  into eq. (2), we get

$$\text{rot}\left(\frac{1}{\mu}\text{rot}\vec{A}\right) = \frac{4\pi}{c}\vec{J}, \quad (3)$$

where

$$\vec{B} = \text{rot}\vec{A}. \quad (4)$$

Equation (3) is a nonlinear Poisson equation because  $\mu$  is a function of  $B$ .

Recently several complex computer programs have been developed solving the three-dimensional equation (3) on the largest computers. However, their application to our case cannot be explicitly justified because of a simple geometry of our magnet and large resources of computer time required to run these programs. In the two-dimensional case it is assumed that  $\vec{A}$  and  $\vec{J}$  have only  $z$  component, i.e.,  $A = A_z(x, y)$  and  $J = J_z(x, y)$ . Equation (3) is then reduced to one differential equation

$$\frac{\partial}{\partial x}\left(\frac{1}{\mu}\frac{\partial A}{\partial x}\right) + \frac{\partial}{\partial y}\left(\frac{1}{\mu}\frac{\partial A}{\partial y}\right) + \frac{4\pi}{c}J = 0. \quad (5)$$

The magnetic field distribution  $B(x, y)$  is obtained from the solution  $A(x, y)$  using expression (4)

$$|\vec{B}| = |\text{rot}\vec{A}| = \sqrt{\left(\frac{\partial A}{\partial x}\right)^2 + \left(\frac{\partial A}{\partial y}\right)^2}. \quad (6)$$

There are several computer programs to solve numerically the nonlinear differential equation (5)<sup>3/</sup>. To obtain the field map in the NA-4 toroidal magnet, we used the program POISSON originally developed at LRL and adopted at JINR<sup>4/</sup>. The principle of solution is to replace the differential equation by a finite system of difference equations, each being approximately valid in the vicinity of a point of a triangular mesh. Using an iterative procedure, the program finally reaches the solution of the original Poisson equation to a given accuracy.

The condition for the application of two-dimensional programs is to have transverse dimensions respectively smaller than longitudinal ones. In our case this is not fulfilled because of the presence of air gaps between the adjacent iron discs. However, it has been shown from the comparison of calculations with direct measurements and from indirect "beam in" experiments that the accuracy guaranteed by a two-dimensional program is sufficient.

The main task of user of the program POISSON is to transform the geometry of all media with different magnetic properties into coordinates of the triangular mesh. As in practice the geometry of the magnet is complex, the other task is to develop a suitable simplified geometrical model.

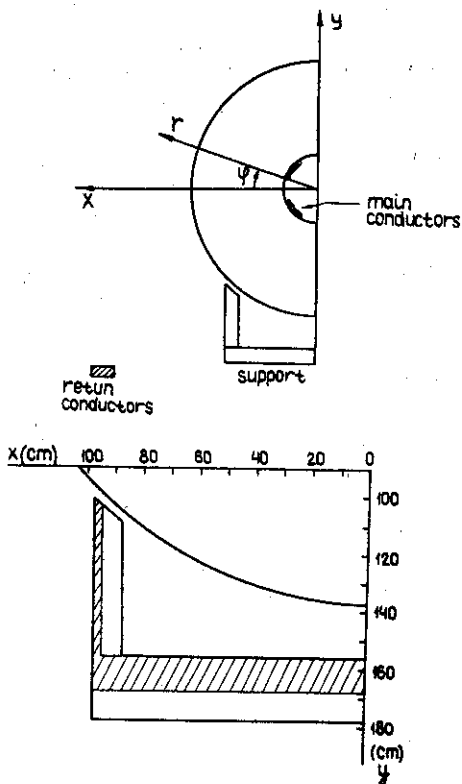


Fig.5. Coordinate system and geometry of the magnet used in calculations. In the lower part are given the geometrical models GEOM1 (shaded) and GEOM2 (full line) of the support.

## 5. GEOMETRICAL MODEL

To solve two-dimensional Poisson equation (5) by the program POISSON, we used the following geometrical model (see Fig.5) in the plane  $(x,y)$ .

Due to the symmetry of our spectrometer, we could perform calculations only in the halfplane  $x \geq 0$  using the boundary condition  $B_y = 0$  at  $x = 0$ . A bunch of six conductors at the  $45^\circ$  diagonals was approximated by one conductor of the equivalent cross section and a total current of + 15000 A. Equivalently 12 return conductors were approximated by one conductor with a total current of 30000 A. To get a better space resolution in iron at small  $r = \sqrt{x^2 + y^2}$ , we always made two calculations, one for regular mesh of a mean area of 24.5 cm /triangle, the other for irregular mesh, more dense at an interval of  $25 \leq r \leq 60$  cm, of a mean area of 10.2 cm /triangle and respectively with larger triangles at  $r > 60$  cm. Due to the size of the CDC 6500 memory, we were limited by 1170 triangles in iron.

The profiled support of the toroid (it corresponds to the dependence in geometry) has been treated in two ways referred to as GEOM1 and GEOM2. Model GEOM1 consists of a thin leg 2.5 cm wide standing on a solid iron base 12 cm thick. In GEOM2 the leg is 10 cm wide and the base 22 cm thick corresponding to real dimensions. To take into account the profiled structure, we introduced filling factors of 0.25 for the leg and 0.51 for the base. A 3 cm air gap corresponding to the stainless plate is left between the toroid and the leg.

## 6. FIELD IN TOROID

As the output of the program POISSON we get the magnetic field map in components  $B_x$ ,  $B_y$ , in iron averaged over a triangle. Without taking into account the toroid support the magnetic field in iron has a radial dependence only. We have checked that the return current conductors have no influence on the magnetic field in the toroid. The main conductors on the inner surface of the toroid do not also disturb a pure radial dependence of the field up to an accuracy of the POISSON results in iron. Starting from the field inside the magnet hole, it will be shown that there exists a small azimuthal dependence of  $\vec{B}$  as an effect of coil reflection in iron. However, the magnitude of this effect is too small to be taken into account in our final results.

Fig.6. The radial dependence  $B_t(r)$  of the field in the toroid without support. The curve is a fit to a third degree polynomial.

The  $B_x$ ,  $B_y$  components are expressed in terms of normal  $B_n$  and tangential  $B_t$  components by the relations

$$B_x = B_n \cos \phi - B_t \sin \phi, \quad (7)$$

$$B_y = B_n \sin \phi + B_t \cos \phi.$$

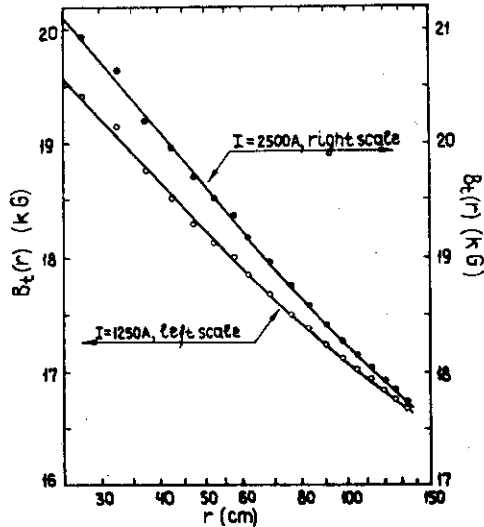
Decomposing  $B_x$  and  $B_y$  into  $B_t$  and  $B_n$  components, we found that the value of the normal component is compatible with the inaccuracy arising from the field averaging procedure in POISSON. Therefore the field in iron is purely toroidal ( $B_n = 0$ ) and depends on  $r$  only. We fitted the  $B_t(r)$  dependence by a third degree polynomial

$$B_t(r) = \sum_{i=0}^3 a_i r^i. \quad (8)$$

The results are shown in Fig.6 and the Table. For comparison we present results for a current of 1250 A per conductor which gives a field about 1.5 kG lower only.

Due to the numerical solution of the Maxwell equation (5), the field map can have a certain error. We estimated it calculating the dispersion of the field in different triangles at fixed  $r$ . The relative error obtained in this way,  $\Delta B/B$ , is 1.5% at  $r = 25$  cm decreasing smoothly to 0.5% at  $r = 137.5$  cm.

The support of the toroid is the main perturbation to the pure radial dependence of  $B_t$  and brings an additional  $\phi$  dependence. The field branches out into the support and brings down the field by a  $\phi$  dependent multiplicative factor in the whole sector between the legs. As the support reduces the





Table

Values of coefficients  $a_i, b_i$  in the polynomial dependence  $B_t(r, \phi)$

$B_t(r) = \sum a_i r^i$		$b_t(\phi) = \sum b_i \sin^i \phi$				
$a_0$ (kG)	23.397 <u>+0.118</u>	$b_0$	1.004	1.167 <u>+0.026</u>	1.006	1.336 <u>+0.033</u>
$a_1$ (kGcm <sup>-1</sup> )	-1.1198 <u>+0.0529</u>	$b_1$	0.0	0.3675 <u>+0.0610</u>	0.0	0.7455 <u>+0.0764</u>
$a_2 \cdot 10^4$ (kGcm <sup>-2</sup> )	8.566 <u>+0.713</u>	$b_2$	0.0	0.1853 <u>+0.0353</u>	0.0	0.3872 <u>+0.0442</u>
$a_3 \cdot 10^6$ (kGcm <sup>-3</sup> )	2.519 <u>+0.295</u>		$\sin \phi \geq$	$\sin \phi <$	$\sin \phi \geq$	$\sin \phi <$
			-0.6741	-0.6741	-0.6934	-0.6934
			GEOM1		GEOM2	

magnetic resistance of the toroid correspondingly, the field becomes slightly higher in the rest of the toroid. To see this effect quantitatively, we plotted in Fig.7 the averaged value of  $B_t(r, \phi)$  over  $r$  for the solutions with an without support. In the lower part of the figure the ratio  $b_t(\phi)$  of fields in the toroid with and without support clearly manifests the shunting effect of support. The loop measurements of the averaged field shown by crosses in Fig.7 are in good agreement with the calculations.

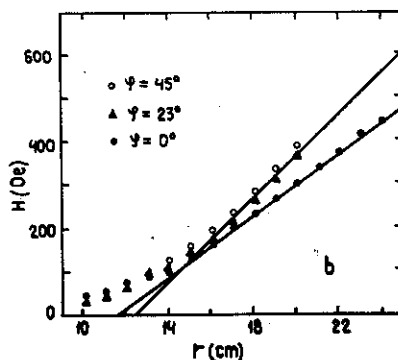
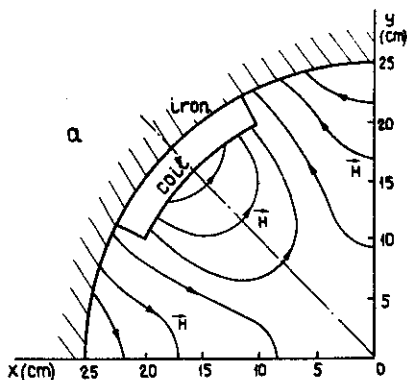
We approximated  $b_t(\phi)$  by a second degree polynomial

$$b_t(\phi) = \sum_{i=0}^2 b_i \sin^i \phi, \quad \sin \phi = \frac{y}{r}, \quad (9)$$

where coefficients  $b_i$  are given in the Table. Thus, the tangential component of the field in the toroid is expressed as a product of two polynomials (8) and (9)

$$B_t(r, \phi) = B_t(r) \cdot b_t(\phi). \quad (10)$$

Fig.7. The dependence of the field averaged over radius  $\bar{B}_t(\phi)$  (upper part). Full squares stand for the toroid without support, full circles (triangles) stand for the support of geometry GEOM1(GEOM2). In the lower part is given the ratio  $b_t(\phi)$  of the field in the toroid with support to that without support. The curve is the result of the second degree polynomial fit in  $\sin \phi$ . Crosses in the upper part show the result of field measurements.



The flow of the field into the support leads to the appearance of a normal component of field  $B_n$ . It is difficult to obtain a small  $B_n$  component directly from the POISSON calculations. As mentioned above, averaging of the field over a triangle of the mesh brings by itself a virtual  $B_n$  component even for a pure radial field. The magnitude of the virtual  $B_n$  component depends on the shape and the area of triangle. The actual  $B_n$  component is obtained by subtraction of  $B_n$  components of fields in the toroid with and without support. The result is shown in Fig.8. We see that  $B_n$  is about zero anywhere except a narrow strip between the toroid axis and support joints. The magnitude of  $B_n$  depends on a model of support geometry. It is larger for a wider and profiled support leg. The result which can be tested by a simple measurement is that the  $B_n$  component at the outer edge of an iron disc is less than 0.2 kG. For practical reasons we fitted the  $B_n(r, \phi)$  dependence by a high degree polynomial in  $r$  and  $\phi$ .

The flow of the field into the support leads to the appearance of a normal component of field  $B_n$ . It is difficult to obtain a small  $B_n$  component directly from the POISSON calculations. As mentioned above, averaging of the field over a triangle of the mesh brings by itself a virtual  $B_n$  component even for a pure radial field. The magnitude of the virtual  $B_n$  component depends on the shape and the area of triangle. The actual  $B_n$  component is obtained by subtraction of  $B_n$  components of fields in the toroid with and without support. The result is shown in Fig.8. We see that  $B_n$  is about zero anywhere except a narrow strip between the toroid axis and support joints. The magnitude of  $B_n$  depends on a model of support geometry. It is larger for a wider and profiled support leg. The result which can be tested by a simple measurement is that the  $B_n$  component at the outer edge of an iron disc is less than 0.2 kG. For practical reasons we fitted the  $B_n(r, \phi)$  dependence by a high degree polynomial in  $r$  and  $\phi$ .

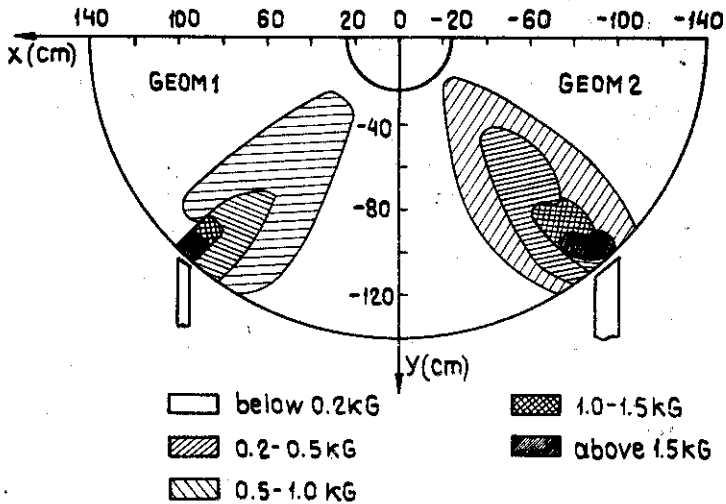


Fig.8. The distribution of the  $B_n$  component in the toroid for GEOM1 and GEOM2 geometry of the support.

## 7. FIELD IN AIR

Due to the coil geometry, the magnetic field in the hole has a complex structure (see Fig.9a). The same field could be generated by an octupole magnetic lens with a current of both polarities and respectively smaller intensities. As is known from the beam optics, the multipole lenses have a focusing effect. Therefore the weak magnetic field in the hole will act against the defocusing influence of multiple scattering in the target.

The radial dependence of the field is displayed for three typical  $\phi$  positions  $\phi = 0^\circ, 23^\circ, 45^\circ$  in Fig.9b. It appears that the field is smaller than 100 Oe at  $r < 14$  cm. Then it increases almost linearly to the iron edge. It is obvious that the field at  $0^\circ, 45^\circ$  has only a tangential component while the field at  $23^\circ$  has mainly a normal component.

The field in air discussed up to now has been obtained for the toroid without support. The support introduces a small disturbance to the field which makes it 50 Oe weaker (stronger) on the side close to (far from) the support compared to

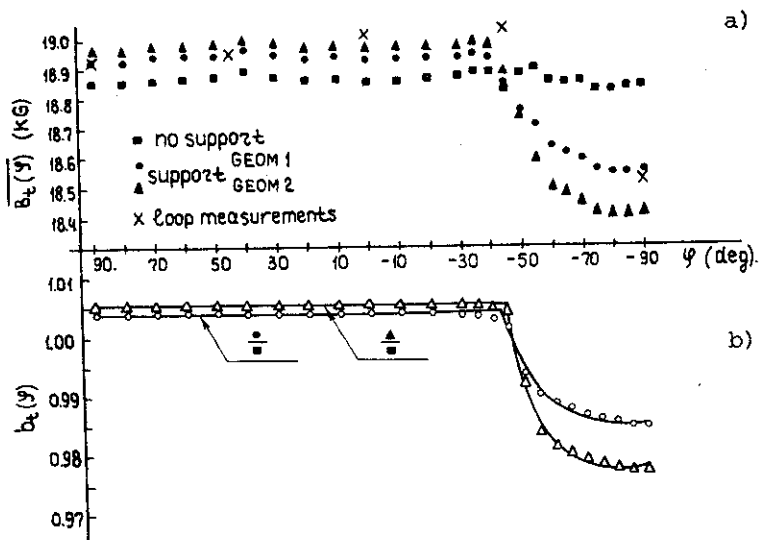


Fig.9. a) The field lines in the hole inside the toroid. b) The  $r$  dependence of the field in the hole at three positions. Lines show an approximate linear increase of the field with radius  $r$ .

the field without support. It has been checked that a relatively weak field in the hole can be ignored in the programs used for the reconstruction of muon tracks in the toroidal spectrometer.

The analysis of the field in the hole gives an indication of the effect of coil geometry on the field in iron at  $r \sim 25$  cm. In the sectors between the conductors the tangential component  $B_t$  is slightly reduced due to the flow of the field from iron into the hole and because of the  $B_n$  component appearing in the hole. This effect not observed directly in field calculations in iron, has been neglected in the field formula (10).

## 8. CONCLUSIONS

The calculations of magnetic field in the NA-4 muon spectrometer provided the magnetic field map for the reconstruction program. The field in iron is toroidal and decreases approximately logarithmically from 21.1 kG at the inner edge to

17.7 kG at the outer edge. The support of the magnet introduces a small disturbance at a level of 2% in the lower part of the magnet. A flow of the field through the support introduces a normal component of field in a narrow sector around the support leg. The multipole field in the hole has been neglected in the reconstruction program presently used.

#### REFERENCES

1. CERN-Dubna-München-Saclay Collaboration, proposal CERN/SPSC/74; 79/SPSC/P19, 1 August 1974; Addendum CERN/SPSC/77-12/SPSC/P19. Add.4, 17 February 1977 (unpublished).
2. Kuchtin V.V. Memorandum to NA-4 collaboration, 25 September 1978.
3. Brechna H. Superconducting Magnet Systems. Springer Verlag, Berlin-Heidelberg, 1973.
4. Vorozhtsov S.B. et al. JINR, B1-11-12070, Dubna, 1978.

Received by Publishing Department  
on April 1 1980.